DOI: https://doi.org/10.24425/amm.2025.156244

KUANG YEE NG^{©1}, NOORHAFIZA MUHAMMAD^{©1,2*}, MOHD SHUHIDAN SALEH^{©1}, SITI NOOR FAZLIAH MOHD NOOR 63, SHAYFULL ZAMREE ABD. RAHIM 61,2, NUR AMALINA MUHAMMAD⁶, KAMALAKANTA MUDULI⁶, S. GARUS⁶

QUANTITATIVE SEM AND IMAGEJ ANALYSIS OF 3D PRINTED POLYCAPROLACTONE SURFACE ROUGHNESS FOR CORONARY STENT APPLICATIONS

Coronary artery disease (CAD) remains a leading cause of mortality, driving advancements in bioresorbable stents (BRS). While 3D printing enables precise fabrication of such stents, surface roughness remains a critical factor influencing biocompatibility and vascular healing. This study investigates the effects of layer height, nozzle temperature, printing speed and flow rate on the surface roughness of 3D-printed polycaprolactone (PCL) BRS. A novel aspect of this work lies in the application of the ImageJ SurfCharJ plugin to quantify roughness metrics (R_a and R_a) from scanning electron microscopy (SEM) images, which is an approach rarely explored in polymer-based stent research. Statistical analyses using t-tests and ANOVA identified layer height and nozzle temperature as the most significant factors, with 0.2 mm layer height and lower nozzle temperatures yielding relatively smoother surfaces. These findings contribute to the optimisation of FDM printing parameters for enhanced surface quality in PCL-based BRS and support the broader adoption of image-based roughness quantification in biomedical additive manufacturing.

Keywords: Surface roughness analysis; 3D printing parameters; polycaprolactone; coronary stents; greyscale-based surface evaluation

1. Introduction

Coronary artery disease (CAD) continues to be a major global cause of mortality, highlighting the need for effective treatment strategies such as coronary stents. Initially, bare metal stents (BMS) were introduced to maintain vascular patency but their high restenosis rates led to the development of drug-eluting stents (DES), which significantly mitigated in-stent restenosis (ISR) through controlled drug release. Despite these advancements, concerns regarding long-term biocompatibility and late stent thrombosis (LST) have driven research toward bioresorbable stents (BRS), which gradually degrade after fulfilling their mechanical support function within the vessel [1]. Among various biodegradable materials, polycaprolactone (PCL) has emerged as a potential candidate due to its suitable mechanical properties, biocompatibility, tunable degradation rate and processability, making it suitable for BRS fabrication [2,3].

To meet the evolving demands of BRS, the fabrication of coronary stents has increasingly shifted from traditional lasercutting techniques to advanced additive manufacturing (3D printing) methods. While laser cutting has been widely used in stent production, it induces thermal damage, leading to microcracks, residual stress and localised material degradation, which may compromise mechanical integrity and biocompatibility [4,5]. In contrast, 3D printing offers enhanced design flexibility, precise material deposition and improved control over microstructural properties. Consequently, 3D printing technology, particularly fused deposition modelling (FDM) technology, has gained attention as a promising alternative for producing customized BRS with optimised properties.

As a promising method for coronary stent fabrication, FDM's effectiveness strongly depends on the precise control of printing parameters, particularly due to their influence on surface roughness, a key factor in determining stent performance

Corresponding author: noorhafiza@unimap.edu.my



UNIVERSITI MALAYSIA PERLIS. FACULTY OF MECHANICAL ENGINEERING & TECHNOLOGY, 02600 ARAU, PERLIS, MALAYSIA

UNIVERSITI MALAYSIA PERLIS, GEOPOLYMER AND GREEN TECHNOLOGY, CENTRE OF EXCELLENCE GEOPOLYMER AND GREEN TECHNOLOGY, 02600 ARAU, PERLIS, MALAYSIA UNIVERSITI SAINS MALAYSIA, DENTAL STIMULATION AND VIRTUAL LEARNING, RESEARCH EXCELLENCE CONSORTIUM, ADVANCED MEDICAL AND DENTAL INSTITUTE, 13200 KEPALA BATAS, PULAU PINANG, MALAYSIA

UNIVERSITI SAINS MALAYSIA, ENGINEERING CAMPUS, SCHOOL OF MECHANICAL ENGINEERING, 14300 NIBONG TEBAL, PULAU PINANG, MALAYSIA

PAPUA NEW GUINEA UNIVERSITY OF TECHNOLOGY, MECHANICAL ENGINEERING DEPARTMENT, LAE, MOROBE PROVINCE. PMB 411. PAPUA NEW GUINEA

CZESTOCHOWA UNIVERSITY OF TECHNOLOGY, FACULTY OF MECHANICAL ENGINEERING, DEPARTMENT OF MECHANICS AND FUNDAMENTALS OF MACHINERY DESIGN, 73 DĄBROWSKIEGO STR., 42-201 CZĘSTOCHOWA, POLAND

and biocompatibility [6]. Previous studies have shown that excessive surface roughness may trigger platelet adhesion and thrombus formation, while an excessively smooth surface may hinder endothelial cell attachment and impede early endothelialisation [7,8]. At the cellular level, surface roughness provides essential topographical cues for endothelial cells. For instance, nanoscale surface features can guide filopodia extension into micro- and nano-scale pores, promoting initial cell anchorage. Moreover, increased surface area from rougher textures enhances protein adsorption, which facilitates integrin-mediated cell adhesion [9]. However, to minimise the risk of adverse vascular responses caused by excessively rough surfaces, a relatively low surface roughness with mean roughness (R_a) of less than 0.5 µm has been identified as one of the desirable design features for coronary stents to improve overall vascular compatibility [10]. Thus, a balance in roughness of coronary stent is needed to support endothelialisation but not so high as to increase thrombogenicity.

Consequently, growing research efforts have focused on optimising surface roughness in FDM-printed structures. Altan et al. [11] found that reducing layer height improved surface quality by 12% in poly(lactic acid) (PLA). Kandi and Pandey [12] optimised infill density, layer height and printing speed, achieving a PCL/polyurethane (PU) tubular scaffold with a surface roughness of 1.85 µm. Ouazzani et al. [13] showed that printing speed, layer height and extrusion temperature influenced acrylonitrile butadiene styrene (ABS) roughness, ranging from 7.18 to 13.4 µm. These studies collectively demonstrated that tuning FDM parameters can effectively improve surface roughness of different materials and potentially enhance downstream performance, including accelerating endothelialisation in vascular applications. However, despite growing interest, limited research has addressed the surface roughness characteristics of BRS particularly fabricated using PCL, highlighting a critical gap that this study aims to fill.

In terms of roughness evaluation, while contact-based profilometry has been widely used, it may not be suitable for microscale or delicate biomaterials. As a result, image-based roughness quantification using scanning electron microscopy (SEM) and the SurfCharJ plugin in ImageJ software has gained popularity, particularly in the field of biomedical implants such as titanium dental implants [14-16], where it has been widely adopted to extract roughness parameters like R_a and root mean square roughness (R_a) . This method offers a non-contact, costeffective alternative to conventional profilometry and has proven effective in assessing the surface texture of various biomaterials. In the context of coronary stents, SurfCharJ has been previously applied by Saqib et al. [17] to analyse the surface roughness of stainless steel stents treated with laser-induced periodic surface structures (LIPSS). Their study demonstrated that increased microscale surface roughness supported endothelial cell adhesion and migration, contributing to improved endothelialisation and potentially reducing late stent thrombosis and restenosis. However, the application of SurfCharJ for quantifying the surface roughness of polymeric BRS remains unexplored.

Building upon the demonstrated utility of SurfCharJ in biomedical surface analysis, this study applies the method for the first time to quantify SEM-derived surface textures of FDM-printed PCL BRS. The aim is to establish a foundational understanding of how extreme variations in key printing parameters affect surface roughness in PCL-based stent structures. The findings are expected to provide valuable insights for optimising printing processes and enhancing the biocompatibility and clinical performance of polymeric BRS.

2. Materials and methods

2.1. Materials

PCL was used as the base material for sample fabrication. The PCL filament utilised has a diameter of 1.75±0.05 mm with an average molecular weight of 50,000 g/mol. PCL was chosen due to its mechanical properties, biocompatibility, biodegradability and suitability for 3D printing and coronary stent applications [3,18,19]. No additional additives or modifications were introduced to the PCL filament to ensure that the results reflect the inherent material properties.

2.2. Sample printing

2.2.1. Printing system

The 3D printing process was conducted using a FDM-based 3D printer (Artillery® Genius Pro, China), equipped with a 0.4 mm nozzle. Stent samples were created using computer aided drawing (CAD) software and processed for printing with Ultimaker Cura slicing software (Ultimaker Cura 5.2.2, Utrecht, Netherlands).

2.2.2. Sample model

Three distinct coronary stent designs were used (Chevron B, Hybrid C and Hybrid A) as illustrated in Fig. 1. These designs were selected based on their demonstrated performance in prior research by Prisipaul et al. [20]. Each stent was fabricated with a strut width of 0.4 mm and a stent thickness of 0.3 mm, dimensions chosen to maintain structural integrity while enabling effective evaluation of surface roughness variations. The inclusion

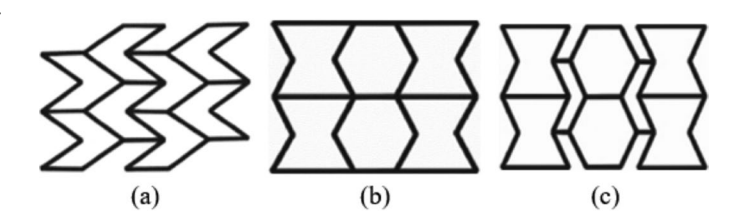


Fig. 1. Stent structure designs: (a) Chevron B, (b) Hybrid C, (c) Hybrid A

of these three designs allows for a comprehensive assessment of how different 3D printing parameters influence surface roughness, ensuring the study's findings are applicable across various stent geometries.

2.2.3. Printing parameters

The experiment employed a One-Factor-At-a-Time (OFAT) approach to systematically investigate the influence of individual FDM parameters on the surface roughness of PCL stent samples. Four key printing parameters were studied: nozzle temperature (80-250°C), printing speed (5-50 mm/s), flow rate percentage (70-150%) and layer height (0.1, 0.2, 0.3 mm). A total of nine parameter combinations were used to fabricate the PCL samples. The parameter ranges were selected based on preliminary experiments conducted using simplified geometries and default slicing software settings. Each parameter was varied individually while keeping the others constant to ensure stable printing and part completion. The chosen ranges also referenced literature sources and considered the melting characteristics of PCL, printer limitations and stent geometry. Specifically, the layer height range was selected to correspond with the 0.3 mm stent thickness designed. To isolate the effect of each parameter, the others were held constant at baseline values: nozzle temperature (165°C), printing speed (27.5 mm/s), flow rate percentage (110%) and layer height (0.1 mm). The bed temperature was maintained at 35°C for all prints.

2.3. Surface roughness analysis

2.3.1. Scanning Electron Microscopy

The surface structure of the PCL stent samples was examined using a tabletop SEM microscope (Hitachi TM3000, Japan) to capture high-resolution images of the sample surfaces. Before imaging, the samples were securely mounted on specimen stubs and coated with a platinum layer via sputter coater (Leica® EM SCD050, USA) to enhance conductivity. SEM imaging was conducted at an accelerating voltage of 10 kV with a magnification of 200×, enabling detailed visualization of surface features for subsequent roughness analysis.

2.3.2. Roughness Index Statistics

Roughness index statistics of the SEM images were conducted using ImageJ software (v1.53t, National Institutes of Health, USA) with the SurfCharJ plugin to quantify surface roughness parameters, including R_a and R_q . The plugin computes these metrics based on the definitions established in ISO 4287/2000. The sampling length used was adjusted according to the study of Mendes et al. [16] and the sampling lengths of 100, 150 and 200 μ m were tested to collect the average R_a

and R_q . The SurfCharJ plugin extracted roughness values from the greyscale intensity variations and the surface plot function was used to generate 3D surface topography representations. Processed images and extracted roughness metrics were exported for statistical analysis, enabling a quantitative assessment of how different 3D printing parameters influence surface roughness in PCL stent samples.

2.4. Statistical analysis

To evaluate the significance of each 3D printing parameter on R_a , two statistical methods were employed using Minitab® 21.4 software (Minitab LLC, State College, PA, USA). An independent samples t-test was performed to assess the effect of nozzle temperature, printing speed and flow rate on R_a , determining whether the differences between parameter variations were statistically significant. Additionally, a one-way analysis of variance (ANOVA) was conducted to assess the effect of layer height on R_a , as this parameter involved multiple levels. All statistical tests were performed at a 95% confidence level ($\alpha = 0.05$).

3. Results and discussion

3.1. Effect of printing parameters on surface roughness based on statistical roughness indices

The R_a and R_q of PCL stent samples were analysed across different nozzle temperature, printing speed, flow rate and layer height (Figs. 2 and 3). The mean roughness values were calculated based on sampling lengths of 100, 150 and 200 μ m, with error bars indicating the variability across these measurements. The results for different stent designs (Chevron B, Hybrid C, Hybrid A) were compared to assess consistency and parameter sensitivity.

The results indicate that nozzle temperature (80 vs. 250°C) exhibits a linear relationship with surface roughness, where both R_a and R_q generally increase at the higher temperature (250°C) across all stent designs. In contrast, the effects of printing speed (5 vs. 50 mm/s) and flow rate (70 vs. 150%) on surface roughness do not display a clear trend. The variations in \mathcal{R}_a and \mathcal{R}_a across different designs suggest that these parameters may have an insignificant influence on surface roughness. The relationship between layer height (0.1, 0.2, 0.3 mm) and surface roughness is nonlinear in all three designs. The highest R_a and R_a values occur at the smallest layer height (0.1 mm). As the layer height increases to 0.2 mm, both roughness metrics decrease significantly, suggesting improved surface uniformity. However, at 0.3 mm, R_a and R_q remain stable or show a slight increase. There is no obvious difference between the influence trends of R_a and R_a , indicating that they are highly correlated.

The findings of this study regarding nozzle temperature are consistent with those reported by Buj-Corral et al. [21,22],

despite the use of PLA instead of PCL. Their studies demonstrated that higher nozzle temperatures led to increased surface roughness, with R_a values reaching up to 18 μ m in one case and 21.77 μ m in another. However, their results were typically observed under conditions combining high nozzle temperature with other contributing factors, such as large nozzle diameter, elevated flow rate, increased layer height and high printing speed. Similarly, Shirmohammadi et al. [23] reported a rise in surface roughness as nozzle temperature increased from 190°C to 210°C. They attributed this trend to the effect of temperature on polymer melting behaviour, which alters the deposition characteristics and promotes surface irregularities.

However, the relationship between layer height and surface roughness observed in this study contrasts with previous findings, which generally suggest that increasing layer height results in higher surface roughness [21-23], including studies focused specifically on PCL-based materials [24]. One possible explanation is that the printed stent samples in this study had a total thickness of only 0.3 mm, which may have introduced constraints that

were not present in previous studies. At a layer height of 0.1 mm, the increased line density and finer deposition features amplify surface irregularities, leading to higher surface roughness. As the layer height increases to 0.2 mm, the deposition of two material layers contributes to a more uniform surface, reducing surface roughness. When the layer height further increases to 0.3 mm, the printed structure consists of only a single deposited layer, which lacks the smoothing effect observed at 0.2 mm. As a result, surface roughness increases again due to the absence of multiple stacked layers that could help refine surface uniformity.

Although no consistent trend was observed in the effects of flow rate and printing speed across the different designs, it is worth noting that both parameters may indirectly influence surface roughness through their impact on layer adhesion. Higher flow rates can lead to over-extrusion [21], potentially enhancing interlayer bonding but also introducing surface irregularities due to excess material deposition. Conversely, higher printing speeds may affect the proper material deposition and interlayer fusion, weakening adhesion and resulting in more pronounced surface

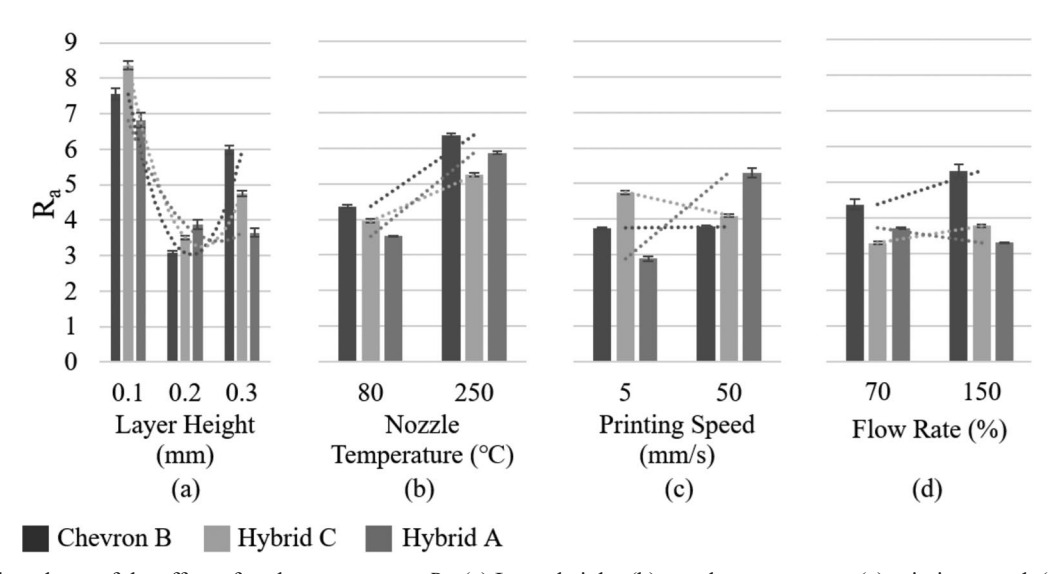


Fig. 2. Grouped bar charts of the effect of each parameter on R_a . (a) Layer height, (b) nozzle temperature, (c) printing speed, (d) flow rate

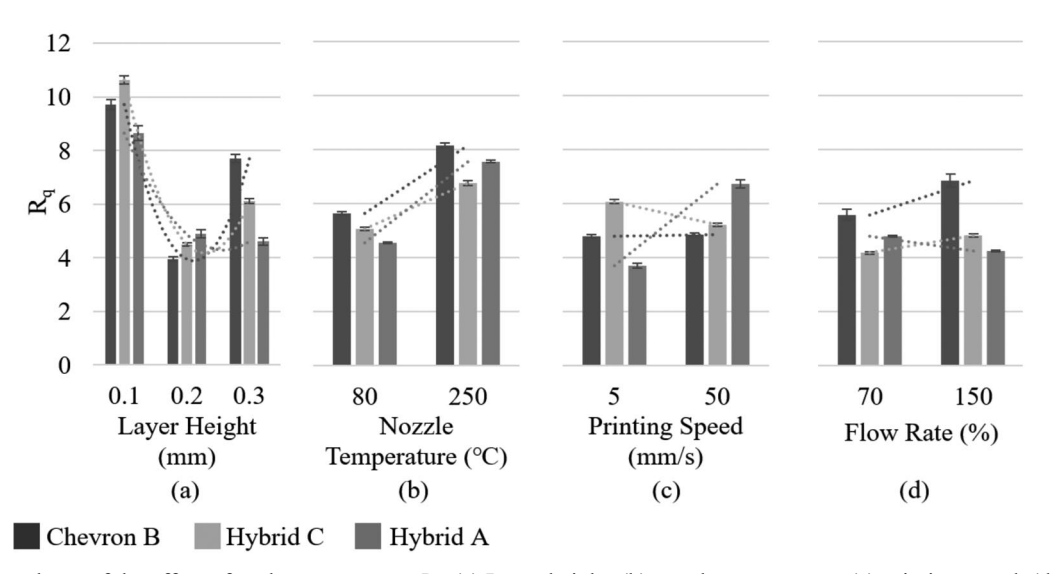


Fig. 3. Grouped bar charts of the effect of each parameter on R_q . (a) Layer height, (b) nozzle temperature, (c) printing speed, (d) flow rate

variations [25]. However, in the present study, such effects did not manifest consistently, possibly due to the small sample thickness (0.3 mm) or the limited number of printed layers.

3.2. Statistical significance of printing parameters on R_a

The statistical analysis results indicate that nozzle temperature and layer height greatly affect R_a , while printing speed and flow rate show no statistically significant effect (TABLE 1). The p-values for nozzle temperature (p=0.000000084) and layer height (p=0.000000010) are well below the standard significance level (p<0.05), confirming their substantial influence. The T-value for nozzle temperature (T=9.22) suggests a strong effect on R_a , while the F-value for layer height (F=69.43) indicates an even greater impact. In contrast, printing speed (p=0.114, T=1.67) and flow rate (p=0.346, T=0.97) have p-values above 0.05, suggesting that their influence on R_a is statistically insignificant. These results highlight that nozzle temperature and layer height are key parameters to consider when optimising the surface quality of coronary stents, as they have the most pronounced effect on surface roughness.

The surface plots further validate the statistical findings regarding the significance of each parameter's influence on surface roughness. Figs. 4 and 5, which present SEM images and corresponding surface plots, illustrate these effects. The white boxes in the SEM images indicate the cropped regions selected

TABLE 1 Statistical Analysis of Printing Parameters on R_a

	p-Value	T-Value	F-Value
Nozzle Temperature	0.000000084	9.22	_
Printing Speed	0.114	1.67	_
Flow Rate	0.346	0.97	_
Layer Height	0.00000000010	_	69.43

for analysis. In the surface plots, the Z-axis represents greyscale-based roughness metrics, with colour variations (blue, purple, red and orange) depicting peaks and valleys at the micron scale. As observed in Fig. 4, the 0.1 mm layer height produces a surface plot with significant colour variations compared to 0.2 mm and 0.3 mm, confirming its substantial impact on surface roughness. Similarly, Fig. 5 demonstrates that nozzle temperature also has a significant effect, as seen in the pronounced differences in surface topography. These findings align with previous studies by Buj-Corral et al. [22] and Taşcıoğlu et al. [26], who also identified layer height as the most critical factor influencing surface roughness.

4. Conclusions

This study demonstrates that layer height and nozzle temperature are the most influential parameters affecting the surface roughness of FDM-printed PCL stent samples. Among

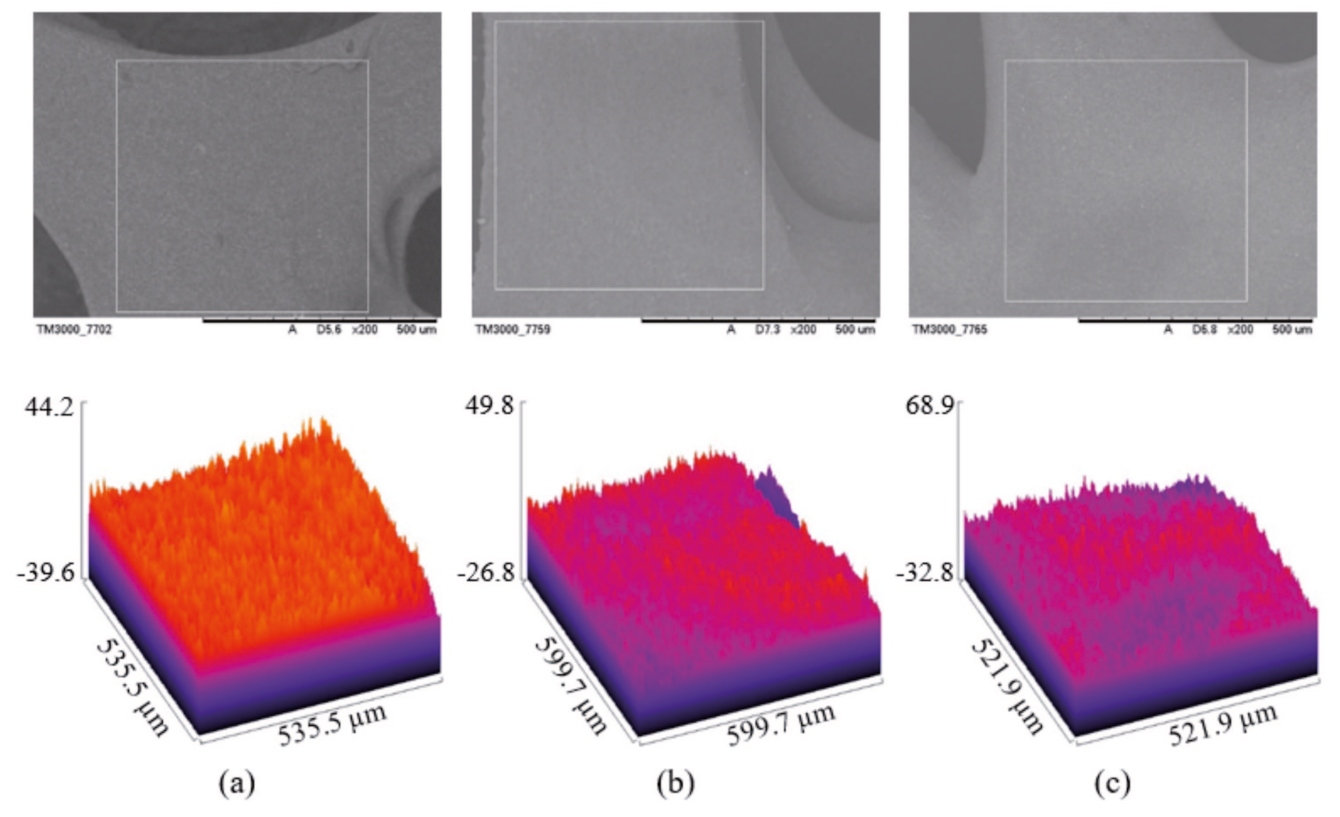


Fig. 4. SEM images and surface plots of the Chevron B design printed with different values of layer height. (a) 0.1 mm, (b) 0.2 mm, (c) 0.3 mm. The surface plots visualize greyscale roughness levels extracted from SEM images, where warmer colours (e.g., red/orange) represent surface peaks and cooler colours (e.g., blue/purple) represent valleys

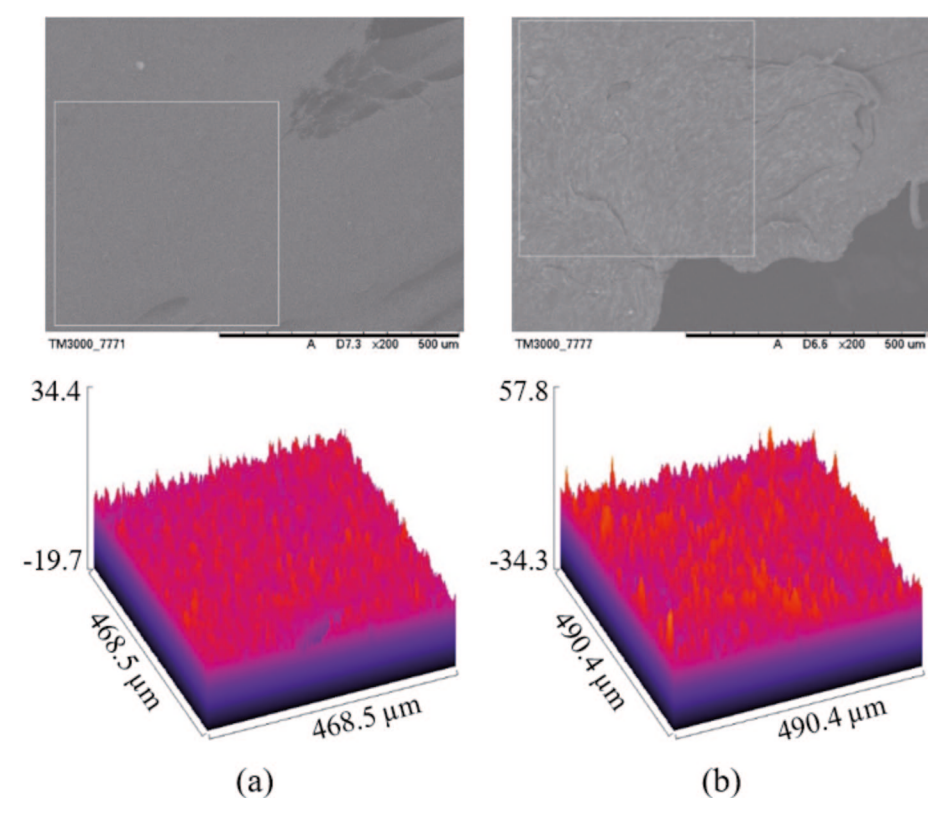


Fig. 5. SEM images and surface plots of the Chevron B design printed with different values of nozzle temperature. (a) 80°C, (b) 250°C. The surface plots visualize greyscale roughness levels extracted from SEM images, where warmer colours (e.g., red/orange) represent surface peaks and cooler colours (e.g., blue/purple) represent valleys

the tested conditions, a layer height of 0.2 mm combined with a lower nozzle temperature resulted in the lowest measured surface roughness values. Therefore, for applications where achieving a R_a below 0.5 µm is desired, which is considered relatively smoother within the context of this study and suitable for coronary stent use, a layer height of 0.2 mm and the lowest practicable nozzle temperature are recommended. The evaluation of surface roughness in this study was conducted using greyscale-based statistical analysis of SEM images via ImageJ and its associated plugins. While these software tools provide a practical and efficient approach for surface roughness assessment, potential limitations or calibration issues may affect their accuracy. This highlights the importance of stringent validation against established measurement techniques to guarantee consistency and dependability of results across approaches. Despite these considerations, the findings provide a useful reference for parameter selection in the fabrication of PCL BRS or similar implantable devices, particularly where surface roughness must be balanced with other critical properties such as dimensional accuracy and mechanical strength.

Acknowledgments

This work was funded by the Fundamental Research Grant Scheme (FRGS) under a grant number of FRGS/1/2021/TK0/UNIMAP/02/19 from Ministry of Higher Education Malaysia.

REFERENCES

- J. Canfield, H. Totary-Jain, 40 years of percutaneous coronary intervention: History and future directions. J. Pers. Med. 8, 33 (2018). DOI: https://doi.org/10.3390/jpm8040033
- [2] S. McMahon, N. Bertollo, E.D.O. Cearbhaill, J. Salber, L. Pierucci, P. Duffy, T. Dürig, V. Bi, W. Wang, Bio-resorbable polymer stents: a review of material progress and prospects. Prog. Polym. Sci. 83, 79-96 (2018).
 - DOI: https://doi.org/10.1016/j.progpolymsci.2018.05.002
- [3] M. Bartnikowski, T.R. Dargaville, S. Ivanovski, D.W. Hutmacher, Degradation mechanisms of polycaprolactone in the context of chemistry, geometry and environment. Prog. Polym. Sci. 96, 1-20 (2019).
 - DOI: https://doi.org/10.1016/j.progpolymsci.2019.05.004
- [4] N. Muhammad, M.M. Al Bakri Abdullah, M.S. Saleh, L. Li, Laser Cutting of Coronary Stents: Progress and Development in Laser Based Stent Cutting Technology. Key. Eng. Mater. 660, 345-350 (2015).
 - DOI: https://doi.org/10.4028/www.scientific.net/kem.660.345
- [5] B. Polanec, J. Kramberger, S. Glodež, A review of production technologies and materials for manufacturing of cardiovascular stents, Advances in Production Engineering and Management 15, 390-402 (2020).
 - DOI: https://doi.org/10.14743/APEM2020.4.373
- [6] A. Jaisingh Sheoran, H. Kumar, Fused Deposition modeling process parameters optimization and effect on mechanical properties

- and part quality: Review and reflection on present research. Mater. Today Proc. ${\bf 21},\,1659\text{-}1672$ (2020).
- DOI: https://doi.org/10.1016/j.matpr.2019.11.296
- [7] C. Lutter, M. Nothhaft, A. Rzany, C.D. Garlichs, I. Cicha, Effect of specific surface microstructures on substrate endothelialisation and thrombogenicity: Importance for stent design. Clin. Hemorheol. Microcirc. 59, 219-233 (2015).
 - DOI: https://doi.org/10.3233/ch-141839
- [8] W. Zhang, Z. Li, C. Xu, M. Chai, P. Dong, Surface characteristics of NiTi cardiovascular stents by selective laser melting and electrochemical polishing. The International Journal of Advanced Manufacturing Technology 130, 623-634 (2024).
 - DOI: https://doi.org/10.1007/s00170-023-12734-x
- [9] A.F. bin A. Fadzil, A. Pramanik, A.K. Basak, C. Prakash,
 S. Shankar, Role of surface quality on biocompatibility of implants
 A review. Annals of 3D Printed Medicine 8, 100082 (2022).
 DOI: https://doi.org/10.1016/j.stlm.2022.100082
- [10] E. Langi, L.G. Zhao, P. Jamshidi, M.M. Attallah, V.V. Silber-schmidt, H. Willcock, F. Vogt, Microstructural and Mechanical Characterization of Thin-Walled Tube Manufactured with Selective Laser Melting for Stent Application. J. Mater. Eng. Perform. 30, 696-710 (2021).
 - DOI: https://doi.org/10.1007/s11665-020-05366-9
- [11] M. Altan, M. Eryildiz, B. Gumus, Y. Kahraman, Effects of process parameters on the quality of PLA products fabricated by fused deposition modeling (FDM): surface roughness and tensile strength. Materials Testing 60, 471-477 (2018).
 DOI: https://doi.org/10.3139/120.111178
- [12] R. Kandi, P.M. Pandey, Statistical modelling and optimization of print quality and mechanical properties of customized tubular scaffolds fabricated using solvent-based extrusion 3D printing process. Proc. Inst. Mech. Eng. H. 235, 1421-1438 (2021). DOI: https://doi.org/10.1177/09544119211032012
- [13] K. Ouazzani, M. El Jai, I. Akhrif, M. Radouani, B. El Fahime, An experimental study of FDM parameter effects on ABS surface quality: roughness analysis. The International Journal of Advanced Manufacturing Technology 127, 151-178 (2023). DOI: https://doi.org/10.1007/s00170-023-11435-9
- [14] F. Ferro, F. Azzolin, R. Spelat, L. Bevilacqua, M. Maglione, Considering the Value of 3D Cultures for Enhancing the Understanding of Adhesion, Proliferation, and Osteogenesis on Titanium Dental Implants. Biomolecules 13, 1048 (2023).
 DOI: https://doi.org/10.3390/biom13071048
- [15] S.J. Perdomo, C.E. Fajardo, A. Cardona-Mendoza, Laminin 332 functionalized surface improve implant roughness and oral keratinocyte bioactivity. Heliyon. 10, e34507 (2024). DOI: https://doi.org/10.1016/j.heliyon.2024.e34507
- [16] G.N. Mendes, L.G. Floresta, W.M. Takeshita, B.F. Brasileiro, C.L. Trento, The Application of ImageJ Software for Roughness Analysis of Dental Implants. Journal of Imaging Informatics in Medicine 38, 1812-1819 (2024).
 - DOI: https://doi.org/10.1007/s10278-024-01298-1

- [17] M. Saqib, N. Beshchasna, R. Pelaccia, A. Roshchupkin, I. Yanko, Y. Husak, S. Kyrylenko, B. Reggiani, G. Cuniberti, M. Pogorielov, J. Opitz, L. Orazi, Tailoring surface properties, biocompatibility and corrosion behavior of stainless steel by laser induced periodic surface treatment towards developing biomimetic stents. Surfaces and Interfaces 34, 102365 (2022).
- [18] R. Dwivedi, S. Kumar, R. Pandey, A. Mahajan, D. Nandana, D.S. Katti, D. Mehrotra, Polycaprolactone as biomaterial for bone
- D.S. Katti, D. Mehrotra, Polycaprolactone as biomaterial for bone scaffolds: Review of literature. J. Oral. Biol. Craniofac. Res. 10, 381-388 (2020).
 - DOI: https://doi.org/10.1016/j.jobcr.2019.10.003

DOI: https://doi.org/10.1016/j.surfin.2022.102365

- [19] F. Koch, O. Thaden, S. Conrad, K. Tröndle, G. Finkenzeller, R. Zengerle, S. Kartmann, S. Zimmermann, P. Koltay, Mechanical properties of polycaprolactone (PCL) scaffolds for hybrid 3D-bioprinting with alginate-gelatin hydrogel. J. Mech. Behav. Biomed. Mater. 130, 105219 (2022). DOI: https://doi.org/10.1016/j.jmbbm.2022.105219
- [20] P.K.M. Prithipaul, M. Kokkolaras, D. Pasini, Assessment of structural and hemodynamic performance of vascular stents modelled as periodic lattices. Med. Eng. Phys. 57, 11-18 (2018). DOI: https://doi.org/10.1016/j.medengphy.2018.04.017
- [21] I. Buj-Corral, A. Bagheri, M. Sivatte-Adroer, Effect of Printing Parameters on Dimensional Error, Surface Roughness and Porosity of FFF Printed Parts with Grid Structure. Polymers (Basel). 13, 1213 (2021). DOI: https://doi.org/10.3390/polym13081213
- [22] I. Buj-Corral, X. Sánchez-Casas, C.J. Luis-Pérez, Analysis of AM Parameters on Surface Roughness Obtained in PLA Parts Printed with FFF Technology. Polymers (Basel) 13, 2384 (2021). DOI: https://doi.org/10.3390/polym13142384
- [23] M. Shirmohammadi, S.J. Goushchi, P.M. Keshtiban, Optimization of 3D printing process parameters to minimize surface roughness with hybrid artificial neural network model and particle swarm algorithm. Progress in Additive Manufacturing 6, 199-215 (2021). DOI: https://doi.org/10.1007/s40964-021-00166-6
- [24] I. Beşliu-Băncescu, I. Tamaşag, L. Slătineanu, Influence of 3D Printing Conditions on Some Physical—Mechanical and Technological Properties of PCL Wood-Based Polymer Parts Manufactured by FDM. Polymers (Basel) 15, 2305 (2023). DOI: https://doi.org/10.3390/polym15102305
- [25] N.A. Sukindar, A.S.H. Md Yasir, M.D. Azhar, M.A. Md Azhar, N.F.H. Abd Halim, M.H. Sulaiman, A.S.H. Ahmad Sabli, M.K.A. Mohd Ariffin, Evaluation of the surface roughness and dimensional accuracy of low-cost 3D-printed parts made of PLA–aluminum. Heliyon 10, e25508 (2024).
 DOI: https://doi.org/10.1016/j.heliyon.2024.e25508
- [26] E. Taşcıoğlu, Ö. Kıtay, A.Ö. Keskin, Y. Kaynak, Effect of printing parameters and post-process on surface roughness and dimensional deviation of PLA parts fabricated by extrusion-based 3D printing. Journal of the Brazilian Society of Mechanical Sciences and Engineering 44, 139 (2022).
 DOI: https://doi.org/10.1007/s40430-022-03429-7